

Extremely local electric field enhancement and light confinement in dielectric waveguide

Qijing Lu,¹ Fang-Jie Shu,² Chang-Ling Zou.^{1,*}

¹ *Key Lab of Quantum Information, University of Science and Technology of China, Hefei 230026, P. R. China*

² *Department of Physics, Shangqiu Normal University, Shangqiu 476000, P. R. China**

(Dated: October 10, 2013)

The extremely local electric field enhancement and light confinement is demonstrated in dielectric waveguide with corner and gap geometry. The numerical results reveal the local electric field enhancement in the vicinity of the apex of fan-shaped waveguide. Classical electromagnetic theory predicts that the field enhancement and confinement abilities increase with decreasing radius of rounded corner (r) and gap (g), and show singularity for infinitesimal r and g . For practical parameters with $r = g = 10$ nm, the mode area of opposing apex-to-apex fan-shaped waveguides can be as small as $4 \times 10^{-3} A_0$ ($A_0 = \lambda^2/4$), far beyond the diffraction limit. This way of breaking diffraction limit with no loss outperforms plasmonic waveguides, where light confinement is realized at the cost of huge intrinsic loss in the metal. Furthermore, we propose a structure with dielectric bow-tie antenna on a silicon-on-insulator waveguide, whose field enhancement increases by one order. The lossless dielectric corner and gap structures offer an alternative method to enhance the light-matter interaction without metal nano-structure, and will find applications in quantum electrodynamics, sensors and nano-particle trapping.

I. INTRODUCTION

Strong light confinement in photonic devices can enhance the light field intensity, and then lead to very strong light-matter interaction. The enhanced light field is essential for a wide range of applications, such as quantum electrodynamics [1, 2], nonlinear optical effect [3], quantum optomechanics [4], optical sensors [5] and nano-optical tweezers [6]. Therefore, the surface plasmon in metal nanostructures is attracting more and more attentions for its unique ability to confine light in the deep subwavelength scale. Extreme strong field enhancements in surface plasmon are mainly attributed to the very small geometry size [7, 8], sharp corners [9–11] and nanoscale gaps [12–14], which has been stated in Ref.[15]. However, intrinsic loss due to internal damping of radiation in metal limits the explosion of practical applications.

For the case of dielectric, light is confined in the wavelength-scale photonic devices, with weak evanescent field interacting with outside. Great efforts have been dedicated to enhance the light field intensity by engineering the dielectric structure. In 2004, Almeida et al. have proposed the dielectric slot waveguide structure, and demonstrated a very effective way to enhance the light field in the void [16, 17]. Very recently, three-dimensional photonic crystal structure has been proposed to guide the light in the wedge-like waveguide with field enhanced at the apex [18]. Actually, the electric field enhancement in the vicinity of the dielectric corner is well known in electrostatics [19]. While in the studies of electromagnetic waves, the corner effect is noticed because it may lead to diffraction at corners and computation difficulties in rectangle-cross-section waveguides [20–22].

In this paper, we numerically demonstrated the extremely local electric field enhancement and light confinement in dielectric waveguide by the corner and gap structures. The waveguide with fan-shaped cross-section is proposed to utilize the corner effect [19–22] to enhance the local electric field, while the opposing apex-to-apex fan-shaped waveguides are studied to apply the gap effect [16, 17]. It is shown that the mode area can be as small as 4×10^{-3} of diffraction limited area for practical geometry, superior to the confinement in hybrid surface plasmon waveguides [23]. Furthermore, we proposed a structure with dielectric bow-tie antenna on a silicon-on-insulator (SOI) waveguide to enhance the amplitude of electric field by one order. It is worth noting that the very sharp corner and closed gap give rise to singularity behavior of local field enhancement, which calls for theoretical efforts to study the quantum effects of dielectric at atomic scale [24–26].

*Electronic address: clzou321@ustc.edu.cn

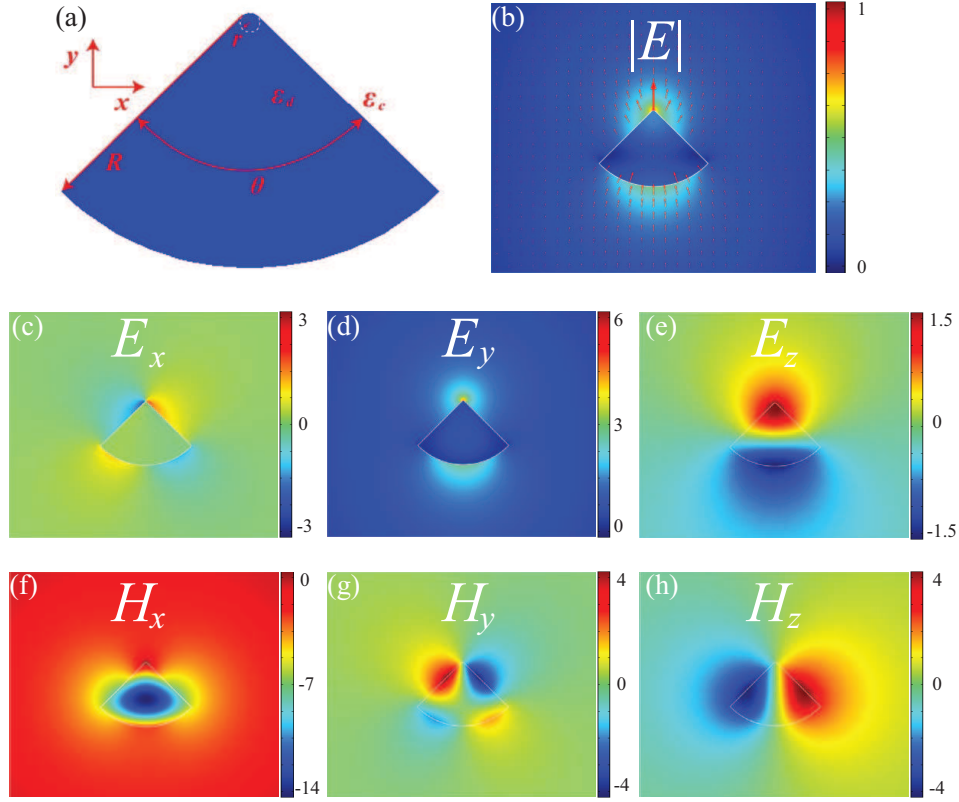


FIG. 1: (a) Schematic illustration of the fan-shaped semiconductor waveguide with a sharp corner. (b) $|E|$ distribution for the fundamental wedge mode. Red arrows indicate the direction of the electric field, which are mainly along the symmetric axis of the fan. (c)-(h) Distributions of electric and magnetic field components E_x , E_y , E_z , H_x , H_y , H_z for the wedge mode. Here, $R = 280$ nm, $r = 10$ nm and $\theta = 90^\circ$.

II. FIELD ENHANCEMENT BY CORNER

First of all, we proposed a fan-shaped waveguide to study the local field enhancement at the dielectric corner. As schematically illustrated in Fig. 1(a), the radius and angle of the fan are R and θ , respectively. Based on practical situations, the apex of fan is rounded corner with radius of curvature r . In our model, the waveguide is made by silicon and embedded in air, with permittivities of waveguide and air cladding being $\epsilon_d = 12.25$ and $\epsilon_c = 1$ at the working wavelength $\lambda = 1550$ nm. All the following results are obtained from the classical electromagnetic theory, which are solved by the Finite Element Method numerically, with commercial available software (COMSOL Multiphysics 4.3).

Figure 1(b) shows the electric field ($|E|$) distribution of the fundamental wedge waveguide mode with $R = 280$ nm, $r = 10$ nm and $\theta = 90^\circ$. Clearly, electric field is greatly enhanced in the vicinity of the apex of fan-shaped waveguide. The polarization of the wedge mode is mainly along the axis of symmetry of fan (i.e. y axis), as indicated by the red arrows. Electric and magnetic field components along x , y , z directions are displayed in Figs. 1(c)-(h), where we can find that only electric field component E_y is enhanced in the vicinity of the apex of corner, showing local electric field enhancement.

In the following, we'll analyze the properties of the wedge modes in detail. Two types of effective mode area of waveguide are introduced to measure the local field enhancement [27]

$$A_e = \frac{\int \int_{all} W_e(\mathbf{r}) d^2 \mathbf{r}}{\max \{W_e(\mathbf{r})\}}, \quad (1)$$

and spatial light confinement [27]

$$A_c = \frac{[\int \int_{all} W_e(\mathbf{r}) d^2 \mathbf{r}]^2}{\int \int_{all} [W_e(\mathbf{r})]^2 d^2 \mathbf{r}}. \quad (2)$$

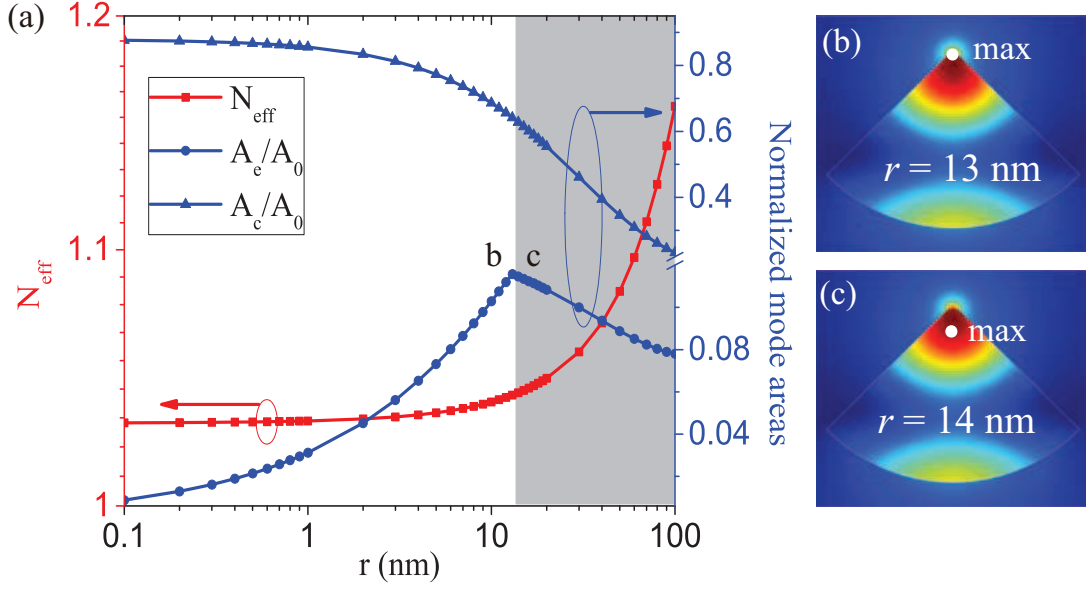


FIG. 2: (a) Dependence of the effective mode index and normalized mode areas on the radius of the curvature r . (b)-(c) Electric energy density W_e when $r = 13$ nm and $r = 14$ nm, respectively. White dots denote the $\max\{W_e(\mathbf{r})\}$. Here, $R = 280$ nm and $\theta = 90^\circ$.

Here $W_e(\mathbf{r})$ is the electric field energy density,

$$W_e(\mathbf{r}) = \frac{1}{2} \varepsilon(\mathbf{r}) |E(\mathbf{r})|^2, \quad (3)$$

with $|E(\mathbf{r})|$ and $\varepsilon(\mathbf{r})$ being electric field and dielectric permittivity, respectively. A_e is more sensitive to $\max\{W_e(\mathbf{r})\}$, and is usually applied to quantify local field enhancement and estimate the enhanced spontaneous emission due to the Purcell effect [27]. A_c characterizes the spatial extent of the field, which is not sensitive to the local field enhancement.

In Fig. 2(a), the effective mode index N_{eff} and normalized mode areas $A_{e,c}/A_0$ are plotted against the radius of rounded corner r , where $A_0 = \lambda^2/4$ denotes the diffraction limited area of vacuum. When r decreases from 100 nm to 0.1 nm, N_{eff} decreases and A_c increases monotonously with opposite trend. Note that N_{eff} also represents the confinement of light field, since strong confinement means more energy confined in dielectric and leads to larger effect mode index. For large r , larger r means larger dielectric cross-section area, so the confinement changes a lot with r . At very small r , the dielectric cross-section area does not change much, so N_{eff} and A_c show saturation when $r < 1$ nm.

On the contrary, A_e increases with decreasing r in the shadow region with $r > 13.5$ nm, similar to A_c , since the cross-section area of dielectric increases. But it decreases with r when $r < 13.5$ nm, with an inflection at $r \approx 13.5$ nm. Carefully comparing the field distributions in the two regimes (see Figs. 2(b) and 2(c) with $r = 13$ nm and $r = 14$ nm), we found that the location of the maximum of the electric energy density ($\max\{W_e(\mathbf{r})\}$) is escaping from the core of the waveguide to the corner as r decreases. For $r < 13.5$ nm, $\max\{W_e(\mathbf{r})\}$ at the corner increases with decreasing r , which shows very strong local electric field enhancement due to the corner structure. Compared to the case of $r = 10$ nm, the mode area A_e for the sharper corner with $r = 0.1$ nm has been reduced to about $1/10$.

In Fig. 3(a), the field confinement is further studied by the energy confinement ratios in silicon (η_1) and air (η_2), where $\eta_{1(2)}$ is defined as the ratio of the electric energy in the silicon (air) to the total electric energy and satisfies $\eta_1 + \eta_2 = 1$. The behavior of η_1 against r agrees well with that of N_{eff} (Fig. 2(a)), since more energy in silicon leads to larger N_{eff} . The curves of A_c , N_{eff} and η_1 indicate that the dielectric corner does not lead to stronger field confinement, but just local electric field enhancement. Insets of Fig. 3(a) are the electric field energy densities for $r = 0.1$ nm and $r = 1$ nm, which demonstrate that the field enhancement is more localized to the corner for smaller r . In Fig. 3(b), the normalized electric fields ($|E|$) along y axis for various r are shown. The field profiles are similar except the enhancement at the corner ($y = 0$), where $|E|$ around the apex decays more drastically for smaller r .

In Fig. 4, the corner effect is studied for different waveguide size R and corner angle θ . For very small R or θ , A_e and A_c are both very large due to the weak confinement of light allowing for the small cross-section area of waveguide. When R or θ increases, N_{eff} increases monotonously, while A_e and A_c decrease first and then slowly increase as the

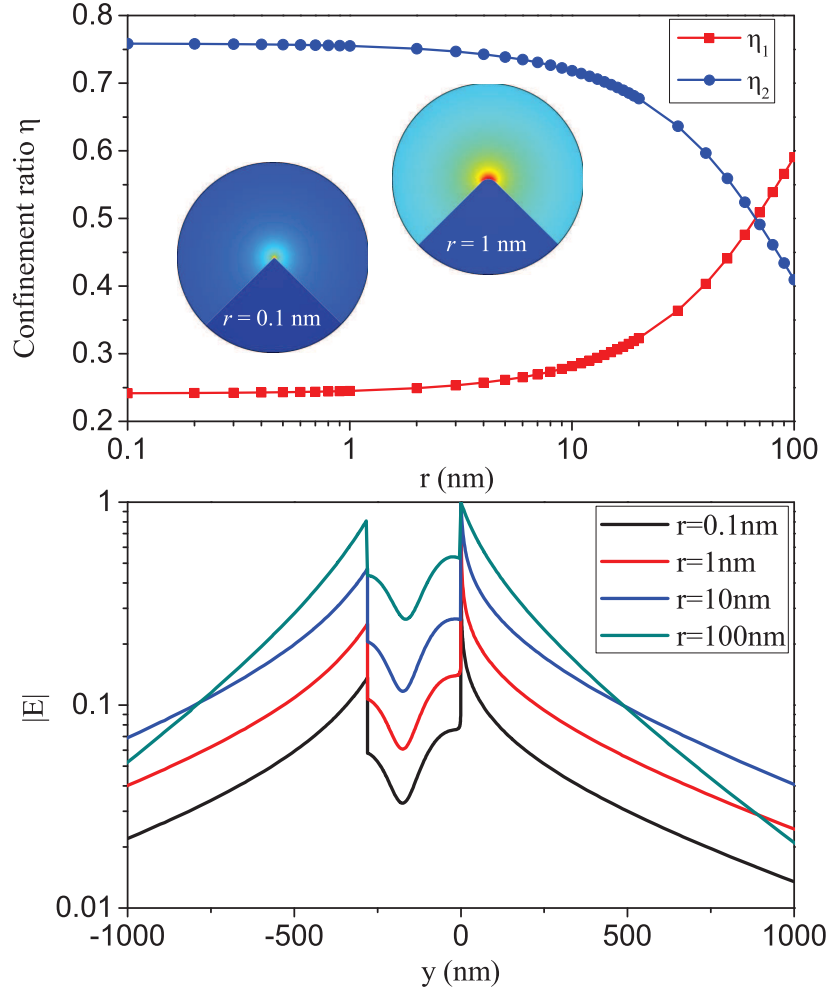


FIG. 3: (a) Electric energy confinement factors in Si (η_1) and air (η_2), respectively. Inset: enlarged view of the $|E|$ distributions of the wedge mode for $r = 0.1$ nm and 1 nm, respectively. (b) Normalized electric density along y axis when $r = 0.1$ nm, $r = 1$ nm, $r = 10$ nm, $r = 100$ nm, respectively.

cross-section area increases. The shadow regions in Fig. 4 correspond to the $\max[\{W(\mathbf{r})\}]$ located inside the dielectric, while the white regions correspond to the local electric field enhanced around the apex of corner. For increasing θ , the wedge mode of fan-shaped waveguide is converted to the channel mode, as shown by the insets in Fig. 4(b).

III. FIELD ENHANCEMENT BY GAP

Gap effect for light enhancement and confinement, caused by large discontinuity of the electric field at high index-contrast interfaces, was studied in Refs. [16, 17], where low-index slot is embedded between two high-index rectangle waveguides. Similar to dielectric slot structures, we can expect further field enhancement in the double fan waveguide posited as apex-to-apex with an air gap g (Fig. 5(a)). As an example shown in Fig. 5(b), we see the very strong field confinement at the gap between the apexes with $g = 10$ nm.

Dependences of the modal characteristics of the gap mode on g are displayed in Figs. 5(c) and 5(d). N_{eff} increases monotonously for decreasing g , because the low-index air surrounding the apex is replaced by high-index dielectric. The trends of N_{eff} with different r are the same, and show saturation for very small gap $g < 1$ nm. For a fixed g , sharper corner gives rise to weaker light confinement in dielectric, which is consistent with the results of single fan-shaped waveguide (Fig. 2(a)). For the mode areas (5(d)), both A_e and A_c show great reduction when reducing the gap. These reveal that the slot structure leads to strong spatial confinement, as well as local field enhancement. However, A_c is saturated when $g < 1$ nm for $r \geq 10$ nm, while A_e is saturated only for $r = 100$ nm. This indicates that the gap effect of apex-to-apex structure also depends on the sharpness of corners.

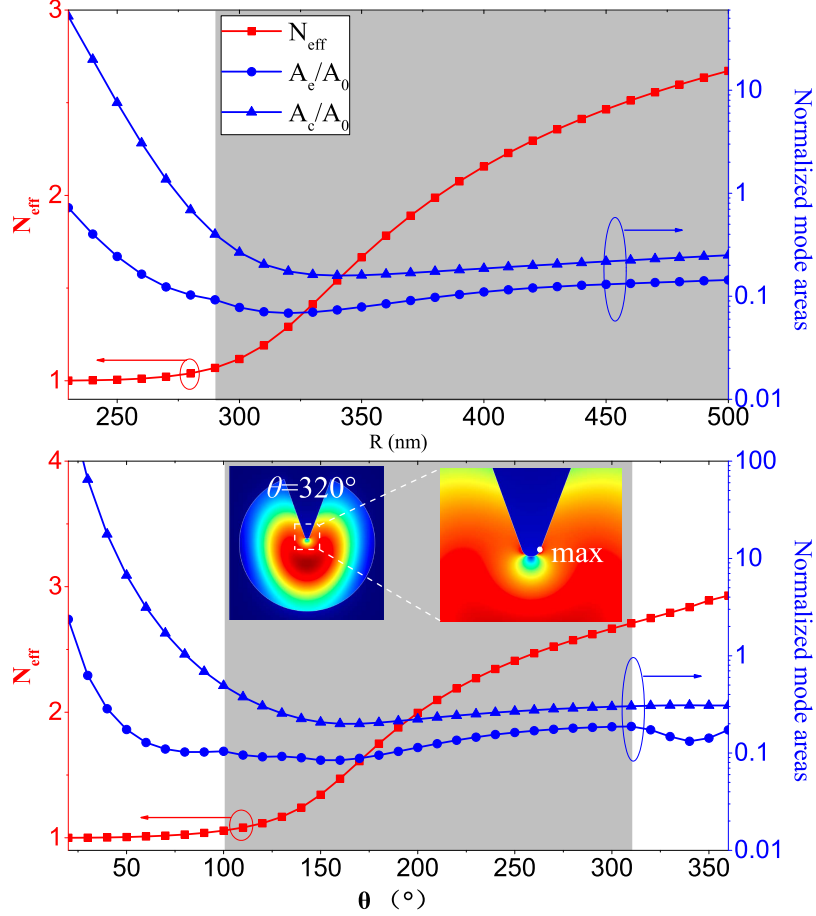


FIG. 4: Dependence of the effective mode index and normalized mode areas on R (a) and θ (b), respectively. Insets in Fig. 4(b) are electric energy density W_e for $\theta = 320^\circ$ and enlarged view of the $\max\{W_e(\mathbf{r})\}$ for $\theta = 320^\circ$.

Due to the combined effects of corner and gap structure, we found that A_e can be as small as $10^{-5}A_0$ for $g = 0.1$ nm and $r = 0.1$ nm. Compared to the best light confinement $A'_e \approx 5 \times 10^{-3}A_0$ in the hybrid dielectric-metal surface plasmon waveguide [23], A_e is 500 times smaller. It is notable that the maximum of electric field is always located at the corner of waveguide, which is very suitable for light to interact with matters outside the dielectric. The extreme light confinement and local electric field enhancement in the dielectric corner and gap would benefit various applications, such as the waveguide quantum electrodynamics, nanoparticle trapping, and bio-sensors.

IV. QUANTUM LIMITATIONS

From the tendency in Fig. 5(d), we can predict that the smaller effective mode area can be obtained by smaller gap or sharper corners. However, when the size of gap or corner structures is reduced to the atomic scale (sub-nanometer), the classical electromagnetic theory will break down and the quantum mechanical effects appear in three aspects:

- (1) The quantum size effect. The object with geometry smaller than atomic scale is meaningless. The sub-nanometer-scale geometry should be treated as atom cluster instead of regular corner or straight boundary. In the atomic scale, the optical response of atomic clusters can not be deduced by the classical dielectric constant of bulk.
- (2) The non-local effect. The atomic-scale wave-function of electrons can spread out from the boundary. Therefore, the response of the electron to electromagnetic wave is no longer local.
- (3) The quantum tunneling. When the gap between two apexes is sub-nanometer, the electrons may tunnel across the gap. Therefore, the electromagnetic field theory for dielectric with zero conductivity is not valid.

These quantum effects in metal nanostructures have been studied extensively recently both in experiments and theoretical studies [24–26]. In theory, the optical responses of those structures at sub-nanometer scale are studied under quantum model with time-dependent density function theory [24], or under semiclassical model with modified

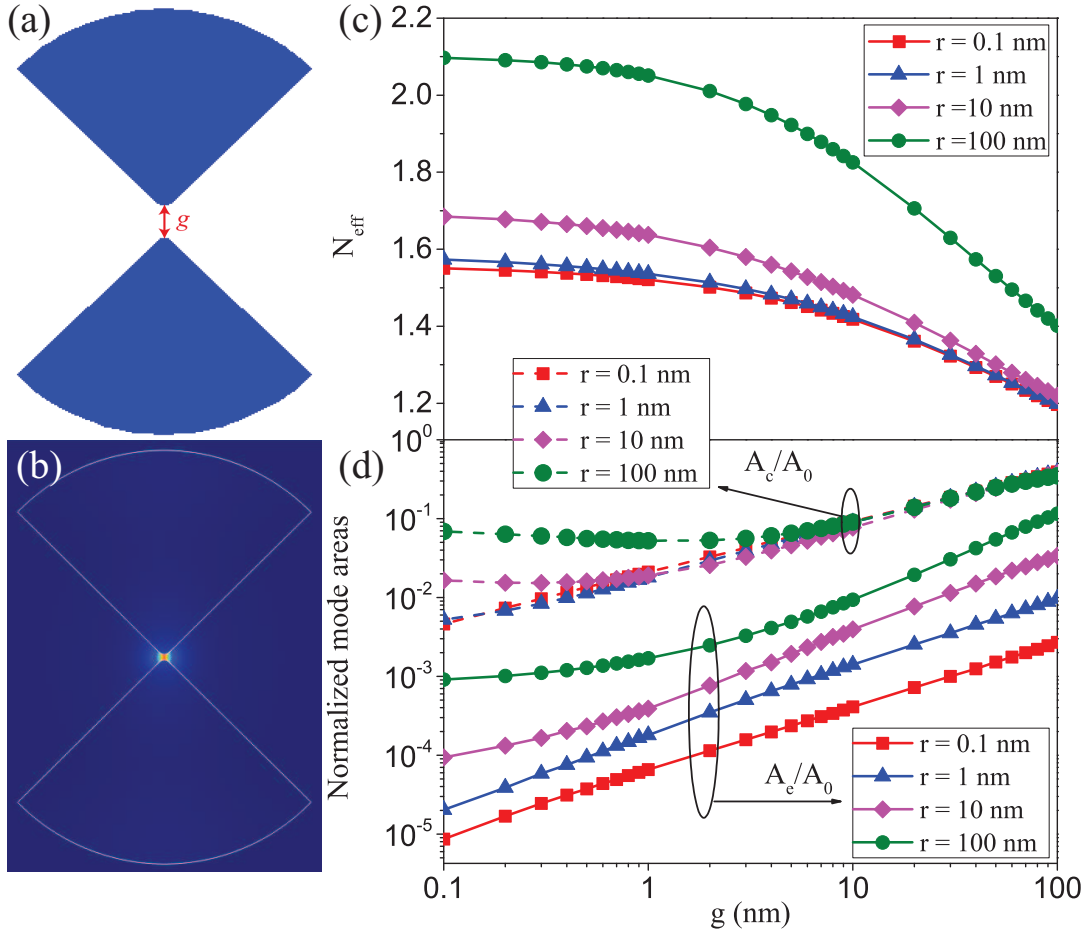


FIG. 5: (a) Schematic of the bow-tie waveguide. (b) Electric energy density W_e of the coupled mode in the bow-tie waveguide for $R = 280$ nm, $r = 10$ nm, $\theta = 90^\circ$ and $g = 10$ nm. N_{eff} (c) and normalized mode areas (d) of the coupled mode as a function of g , for $r = 0.1$ nm, $r = 1$ nm, $r = 10$ nm, $r = 100$ nm, respectively.

electromagnetic theory by including hydrodynamic description of conducting electrons [25, 26]. It is demonstrated that the singular behavior is avoided in those theoretical models and experiments. Therefore, we could also expect the singular behavior to be removed by corrected models. However, the property of electrons in dielectric is significantly different from that in metal, so new models should be developed to study the optical response of the atomic scale dielectric structures.

Although the light confinement and local field enhancement may be limited by quantum effects, the apex-to-apex dielectric structure studied here is still superior to the plasmon waveguides: (a) Optical modes in the apex-to-apex fan waveguides are lossless, which is an incomparable advantage over plasmonic waveguides where light confinement is realized at the cost of huge intrinsic loss in the metal. (b) Even for the case of $g = 10$ nm and $r = 10$ nm where the classical Maxwell equations are valid, we get $A_e \approx 4 \times 10^{-3} A_0$ which is smaller than that of hybrid plasmonic waveguide [23].

V. DIELECTRIC BOW-TIE ANTENNA

The corner and gap effects have been demonstrated above for dielectric waveguides with different cross-section geometry, where light propagates perpendicularly to the cross-section. Now, we turn to study the field enhancement in the dielectric bow-tie (DBT) antenna structure, where the corner and gap structures are not uniform along the waveguide. This DBT antenna can be integrated with various photonic structures, such as waveguide and microring, and is very potential for practical applications.

As shown in Fig. 6(a), a dielectric bow-tie antenna is placed on a silicon-on-insulator (SOI) waveguide with rectangle cross-section of 450 nm \times 250 nm. The bow-tie antenna consists of two opposing apex-to-apex silicon isosceles triangles,

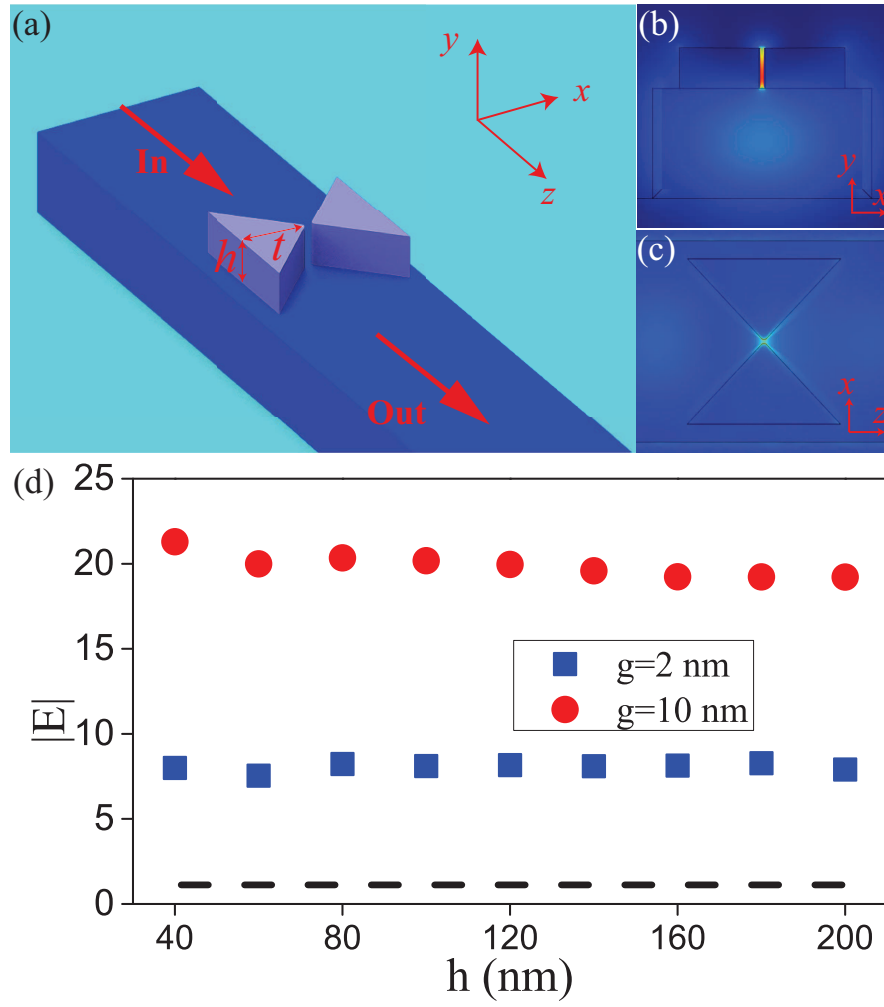


FIG. 6: (a) Schematic of the dielectric bow-tie antenna. Side (b) and top (c) views of the $|E|$ of the dielectric bow-tie antenna. (d) Maximum of $|E|$ at the center of the gap for $g = 2$ nm, $g = 10$ nm, respectively, as a function of h .

the height and thickness of which are denoted as h and t , respectively. The vertex angle of the nano-triangle is 100° , and the radius of the round is $r = 10$ nm. Due to the effects of corner and gap, we can expect a strongly enhanced field in the gap of the DBT antenna. To investigate the field enhancement, the three-dimensional model with 1550 nm fundamental TE-polarized mode loaded in the waveguide is simulated numerically. From the field profiles in Figs. 6(b) and 6(c), the electric field is greatly enhanced in the gap of DBT antenna compared to that in the waveguide. Note that the corner and gap effects can only be expected for the electric field along the axis of symmetry of the corner, and there is no field enhancement for the TM-polarized mode.

In Fig. 6(d), the maximum of $|E|$ at the center of the gap of DBT antenna is plotted as a function of h for $g = 2$ nm and $g = 10$ nm, respectively. The evanescent field of the fundamental TE mode at the top surface of the waveguide without DBT antenna is also shown by the dashed line. We can find that the maximum of $|E|$ is enhanced by 20 and 8 times for $g = 2$ nm and $g = 10$ nm, respectively. In both cases, the enhancement factor is insensitive to h . The narrower gap leads to the stronger electric field enhancement, which is consistent with the results in the apex-to-apex fan waveguides. The DBT antenna is easy for fabrication and compatible with CMOS technology, thus it will be useful as building blocks in integrated photonic circuits.

VI. CONCLUSION

In summary, we demonstrate the corner- and gap-enhanced local electric field in dielectric waveguide. As an example, in opposing apex-to-apex fan-shaped waveguides with $r = g = 10$ nm, the mode area of fundamental wedge mode can be as small as $4 \times 10^{-3} A_0$ ($A_0 = \lambda^2/4$), far beyond the diffraction limit. The numerical results indicate

that the field enhancement and confinement abilities increase with decreasing radius of rounded corner (r) and gap (g), and show singularity for infinitesimal r and g . The singularity behavior calls for theoretical efforts to study the quantum effects of dielectric at atomic scale. Furthermore, we propose a structure with dielectric bow-tie antenna on a silicon-on-insulator waveguide, the field enhancement of which is improved by one order. Although the waveguide studied in this paper is focused at 1550 nm, we should be aware that the corner and gap effects are broadband. The lossless dielectric corner and gap structures offer an alternative method to enhance the light-matter interaction without metal nano-structure, and will find applications in quantum electrodynamics, sensors and nano-particle trapping.

Acknowledgments

We thank Xiao Xiong for discussion. CLZ is supported by the 973 Programs (No. 2011CB921200). FJS is supported by the National Natural Science Foundation of China (No. 11204169 and No. 11247289).

-
- [1] Q. Quan, I. Bulu, and M. Lončar, “Broadband waveguide QED system on a chip,” *Phys. Rev. A* **80** 011810 (2009).
 - [2] K. J. Russell, T.-L. Liu, S. Cui, and E. L. Hu, “Large spontaneous emission enhancement in plasmonic nanocavities,” *Nature Photon.* **6**, 459-462 (2012).
 - [3] S. Spillane, T. Kippenberg, and K. Vahala, “Ultralow-threshold Raman laser using a spherical dielectric microcavity,” *Nature* **415**, 621-623 (2002).
 - [4] D. Van Thourhout, and J. Roels, “Optomechanical device actuation through the optical gradient force,” *Nature Photon.* **4**, 211-217 (2010).
 - [5] J. N. Anker, W. P. Hall, O. Lyandres, N. C. Shah, J. Zhao, and R. P. Van Duyne, “Biosensing with plasmonic nanosensors,” *Nature Mater.* **7**, 442-453 (2008).
 - [6] M. L. Juan, R. Maurizio and Q. Romain, “Plasmon nano-optical tweezers,” *Nature Photon.* **5**, 349-356 (2011).
 - [7] W. L. Barnes, A. Dereux, and T. W. Ebbesen, “Surface plasmon subwavelength optics,” *Nature* **424**, 824-830 (2003).
 - [8] M. A. Noginov, G. Zhu, A. M. Belgrave, R. Bakker, V. M. Shalaev, E. E. Narimanov, S. Stout, E. Herz, T. Suteewong, and U. Wiesner, “Demonstration of a spaser-based nanolaser,” *Nature* **460**, 1110-1112 (2009).
 - [9] D. F. P. Pile, T. Ogawa, D. K. Gramotnev, T. Okamoto, M. Haraguchi, M. Fukui, and S. Matsuo, “Theoretical and experimental investigation of strongly localized plasmons on triangular metal wedges for subwavelength waveguiding,” *Appl. Phys. Lett.* **87**, 061106 (2005).
 - [10] M. Yan and M. Qiu, “Guided plasmon polariton at 2D metal corners,” *J. Opt. Soc. Am. B* **24**, 2333-2342 (2007).
 - [11] E. Moreno, S. G. Rodrigo, S. I. Bozhevolnyi, L. Martín-Moreno, and F. García-Vidal, “Guiding and focusing of electromagnetic fields with wedge plasmon polaritons,” *Phys. Rev. Lett.* **100**, 023901 (2008).
 - [12] A. Sundaramurthy, K. Crozier, G. Kino, D. Fromm, P. Schuck, and W. Moerner, “Field enhancement and gap-dependent resonance in a system of two opposing tip-to-tip Au nanotriangles,” *Phys. Rev. B* **72**, 165409 (2005).
 - [13] S. Kim, J. Jin, Y.-J. Kim, I.-Y. Park, Y. Kim, and S.-W. Kim, “High-harmonic generation by resonant plasmon field enhancement,” *Nature* **453**, 757-760 (2008).
 - [14] A. Kinkhabwala, Z. Yu, S. Fan, Y. Avlasevich, K. Müllen, and W. E. Moerner, “Large single-molecule fluorescence enhancements produced by a bowtie nanoantenna,” *Nature Photon.* **3**, 654-657 (2009).
 - [15] S. Thomas, M. Kruger, M. Forster, M. Schenk, and P. Hommelhoff, “Probing of optical near-fields by electron rescattering on the 1 nm scale,” *Nano Lett.* DOI: 10.1021/nl402407r (2013).
 - [16] V. R. Almeida, Q. Xu, C. A. Barrios, and M. Lipson, “Guiding and confining light in void nanostructure,” *Opt. Lett.* **29**, 1209-1211 (2004).
 - [17] Q. Xu, V. R. Almeida, R. R. Panepucci, and M. Lipson, “Experimental demonstration of guiding and confining light in nanometer-size low-refractive-index material,” *Opt. Lett.* **29**, 1626-1628 (2004).
 - [18] L. Lu, J. D. Joannopoulos, and M. Soljačić, “Waveguiding at the Edge of a Three-Dimensional Photonic Crystal,” *Phys. Rev. Lett.* **108**, 243901 (2012).
 - [19] L. Dobrzynski, and A. Maradudin, “Electrostatic edge modes in a dielectric wedge,” *Phys. Rev. B* **6**, 3810-3815 (1972).
 - [20] C. Bouwkamp, “A note on singularities occurring at sharp edges in electromagnetic diffraction theory,” *Physica* **12**, 467-474 (1946).
 - [21] J. Meixner, “The behavior of electromagnetic fields at edges,” *IEEE Trans. Antennas Propag.* **20**, 442-446 (1972).
 - [22] G. R. Hadley, “High-accuracy finite-difference equations for dielectric waveguide analysis II: Dielectric corners,” *J. Lightw. Technol.* **20**, 1219-1231 (2002).
 - [23] R. F. Oulton, V. J. Sorger, D. Genov, D. Pile, and X. Zhang, “A hybrid plasmonic waveguide for subwavelength confinement and long-range propagation,” *Nature Photon.* **2**, 496-500 (2008).
 - [24] J. A. Scholl, A. L. Koh, and J. A. Dionne, “Quantum plasmon resonances of individual metallic nanoparticles,” *Nature* **483**, 421-427 (2012).
 - [25] C. Ciraci, R. T. Hill, J. J. Mock, Y. Urzhumov, A. I. Fernandez-Dominguez, S. A. Maier, J. B. Pendry, A. Chilkoti, and D. R. Smith, “Probing the ultimate limits of plasmonic enhancement,” *Science* **337**, 1072-1074 (2012).

- [26] L. Stella, P. Zhang, F. J. García-Vidal, A. Rubio, P. García-González, “Performance of Non-local Optics when Applied to Plasmonic Nanostructures,” *J. Phys. Chem. C* **117**, 8941-8949 (2013).
- [27] R. F. Oulton, G. Bartal, D. Pile, and X. Zhang, “Confinement and propagation characteristics of subwavelength plasmonic modes,” *New J. Phys.* **10**, 105018 (2008).